APLP2 regulates neuronal stem cell differentiation during cortical development

S. Ali M. Shariati[1,2], Pierre Lau[1,2], Bassem A. Hassan[1,2], Ulrike Müller[3], Carlos G. Dotti[1,2,4,*], Bart De Strooper[1,2,*] and Annette Gärtner[1,2,*]

[1]KU Leuven, Center for Human Genetics and Leuven Institute for Neurodegenerative Diseases (LIND), 3000 Leuven, Belgium
[2]VIB Center for the Biology of Disease, 3000 Leuven, Belgium
[3]Institute of Pharmacy and Molecular Biotechnology, University Heidelberg, 69120 Heidelberg, Germany
[4]Centro de Biología Molecular Severo Ochoa, CSIC/UAM, C/Nicolás Cabrera 1, Campus de la Universidad Autónoma de Madrid, 28049 Madrid, Spain
*Authors for correspondence (cdotti@cbm.uam.es; Bart.DeStrooper@med.kuleuven.be; Annette.Gaertner@cme.vib-kuleuven.be)

Accepted 14 December 2012
Journal of Cell Science 126, 1268–1277

doi: 10.1242/jcs.122440

Summary

Expression of amyloid precursor protein (APP) and its two paralogues, APLP1 and APLP2 during brain development coincides with key cellular events such as neuronal differentiation and migration. However, genetic knockout and shRNA studies have led to contradictory conclusions about their role during embryonic brain development. To address this issue, we analysed in depth the role of APLP2 during neurogenesis by silencing APLP2 *in vivo* in an APP/APLP1 double knockout mouse background. We find that under these conditions cortical progenitors remain in their undifferentiated state much longer, displaying a higher number of mitotic cells. In addition, we show that neuron-specific APLP2 downregulation does not impact the speed or position of migrating excitatory cortical neurons. In summary, our data reveal that APLP2 is specifically required for proper cell cycle exit of neuronal progenitors, and thus has a distinct role in priming cortical progenitors for neuronal differentiation.

Key words: Amyloid precursor protein, Amyloid precursor-like protein, Cell cycle exit, Neuron migration, Progenitors

Introduction

In mammals, the APP gene family consists of three evolutionary conserved members: amyloid precursor protein (APP), amyloid precursor-like protein (APLP) 1 and APLP2. Although the role of APP as precursor of amyloid beta in the context of Alzheimer's disease is well understood (Reinhard et al., 2005), the physiological role of APP is still largely unclear. Gain and loss of function studies have suggested a role of APP in neuronal migration (Herms et al., 2004; Young-Pearse et al., 2007), cell–cell adhesion (Soba et al., 2005), neurite outgrowth (Leyssen et al., 2005; Young-Pearse et al., 2008), synapse formation and function (Wang et al., 2009; Weyer et al., 2011), intracellular signalling (Cao and Südhof, 2001; Deyts et al., 2012) see however (Hébert et al., 2006), axonal pruning (Nikolaev et al., 2009) and neurogenesis (Aydin et al., 2011; Ma et al., 2008; for reviews, see Müller et al., 2012; Reinhard et al., 2005). Moreover, observations made in different models are sometimes contradictory and argue at first glance for opposing functions for the APP family. For instance, Young-Pearse et al. (Young-Pearse et al., 2007) demonstrated that the downregulation of APP in precursors and neurons of the developing cortex *in vivo* blocks the migration of neurons towards the cortical plate. Conversely, Herms et al. (Herms et al., 2004) had reported that neurons in an APP/APLP1/APLP2 triple knockout (ko) mice overmigrate and accumulate ectopically in the marginal zone (Herms et al., 2004), resembling human type 2 cobblestone lissencephaly. The discrepancy between the overmigration effects in the triple ko (Herms et al., 2004) and the blocked migration in the case of APP downregulation (Young-Pearse et al., 2007) shows that the role of the APP family members in the course of cortical development is still unclear. Alternatively, APP and APLPs may regulate distinct processes in different regions of the developing cortex. Interestingly, mRNA expression data support this idea because APP and APLP1 and APLP2 expression patterns differ in the developing cortex: APP is found in the cortical plate (CP) and ventricular zone (VZ), APLP2 in the VZ and subventricular zone (SVZ) and APLP1 in the CP only (Diez-Roux et al., 2011; López-Sánchez et al., 2005; Visel et al., 2004). The restriction of APLP2 expression to the proliferative zones (VZ/SVZ) of the developing cortex makes it a very interesting candidate for a specific function in the development and specification of cortical progenitors. Therefore we focused our attention on the involvement of APLP2 in cortical development.

To address this question, we silenced, *in utero*, the expression of APLP2 in developing cortices of both wild-type (wt) and APP/APLP1 double knockout (dko) embryos. We investigated the effect of the loss of APLP2 function in the proliferation and differentiation of progenitors, and migration and final positioning of cortical excitatory neurons. Our data reveal that APLP2 is required for proper progression of neuronal differentiation program of cortical progenitors.

Results

APLP2 downregulation in dko cortices affects cortical positioning

To examine the role of APLP2 in cortical development, we used two different U6 driven shRNA constructs targeting different regions of the coding sequence of the APLP2 transcript. Western-blot analysis

of APLP2-V5 overexpressing HEK293 cells which were transfected with one of those shRNA constructs confirmed the downregulation of APLP2 protein (APLP2 shRNA1 more than 95% knockdown and APLP2 shRNA2 more than 80% knockdown; Fig. 1A). Since APLP2 shRNA1 was more efficient for the downregulation of APLP2 protein, we used in most of our analysis this shRNA construct (referred to hereafter as APLP2 shRNA) and utilized the second construct in initial experiments in order to validate the

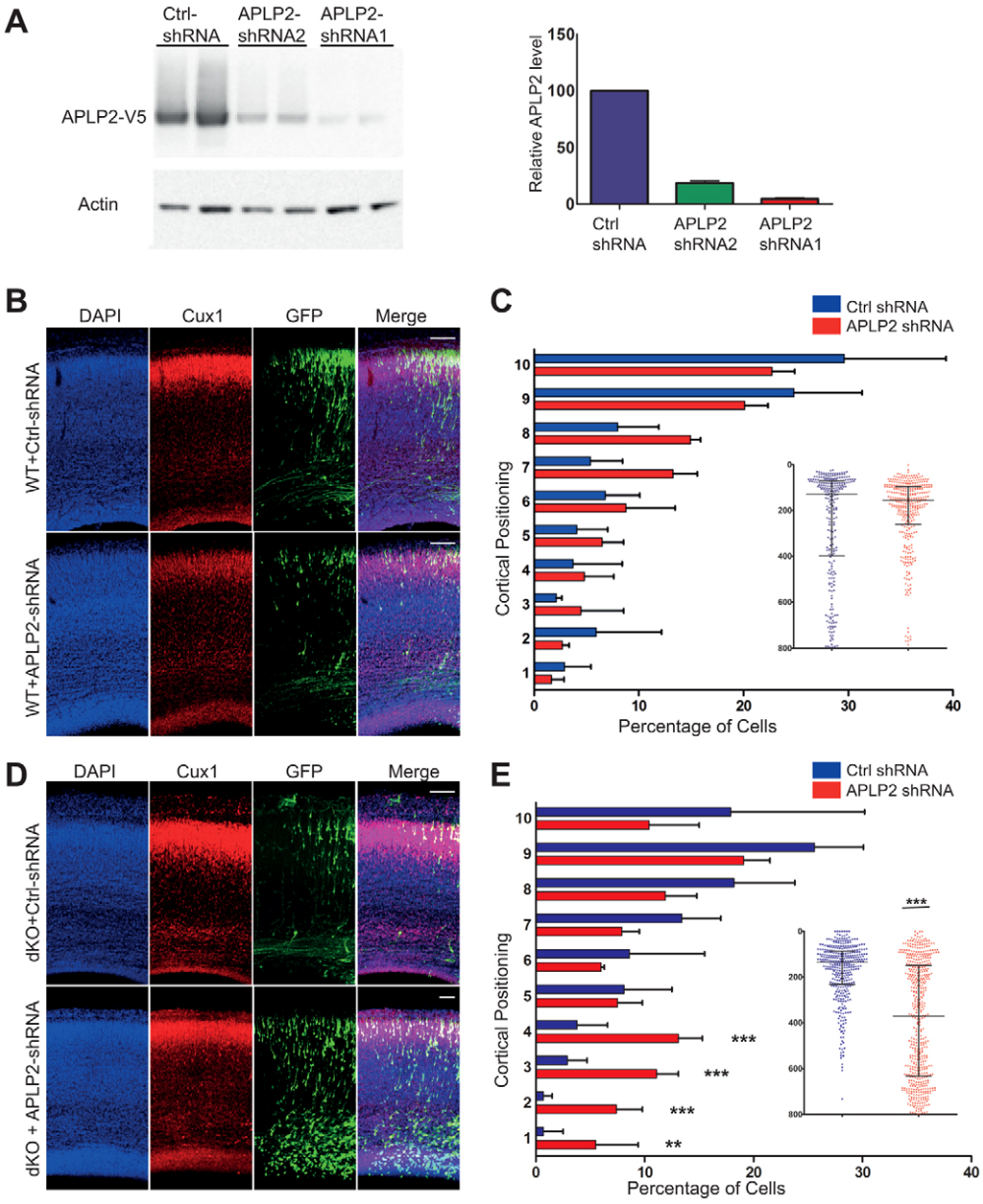

Fig. 1. APLP2 downregulation changes the positioning of cells in dko cortices. (**A**) Left: Western blot showing protein levels of APLP2-V5 and actin (loading control) of HEK cells expressing APLP2-V5 transfected with U6 driven APLP2 shRNA1, APLP2 shRNA2 or control shRNA. Right: downregulation of APLP2 normalized to the total actin (n=4). (**B**) Confocal images of coronal slices of wild-type (WT) brains electroporated with constructs expressing APLP2 shRNA or control shRNA together with EGFP, 4 days after electroporation (E14.5–E18.5). APLP2 shRNA expression does not lead to developmental differences in respect to wild-type conditions. (**C**) Quantification of EGFP-positive cells shown in B. Bar graphs represent frequency distribution of EGFP-positive cells in ten equally divided bins from ventricle (1) to the pial surface (10) of the cortical wall. Values represent the mean ± s.d. (n=5; Student's t-test). The inset scatter plot compares the population distribution of EGFP-positive cells (n=3, only 300–400 cells only are shown for clarity of graph; values represent the median ± interquartile range; Mann–Whitney test). (**D**) Confocal images of APP/APLP1 dko cortices transfected with APLP2 shRNA or control shRNA construct coexpressing EGFP, 4 days after electroporation (E14.5–E18.5). APLP2 shRNA expression alters cortical positioning of dko cells (**E**) Quantification of EGFP-positive cells shown in D. Bar graphs show frequency distribution of EGFP-positive cells in ten equally divided bins from ventricle (1) to the pial surface (10) of cortical wall. Values represent the mean ± s.d. (n=5; Student's t-test). The inset scatter plot compares the population distribution of EGFP-positive cells (n=3, 300–400 cells for clarity of graph; values represent the median ± interquartile range; Mann–Whitney test). All confocal images are maximal intensity projections of 10–15 consecutive z-sections. Upper cortical layers are stained with Cux1 antibody and DAPI is used for nuclear staining. Scale bars: 50 µm. $^{**}P<0.01$, $^{***}P<0.001$.

phenotype and exclude the possibility of off-target effects. Also in cultures of cortical neurons from E14 mice (supplementary material Fig. S2A) and in mouse embryonic fibroblasts (data not shown), endogenous APLP2 expression was clearly downregulated by APLP2 shRNA1 three days after transfection.

To address APLP2 function, we expressed the APLP2 shRNA constructs in cortical progenitors of wt mice at E14.5 by using *in utero* electroporation. APLP2 is highly expressed in the developing cortex at E14.5 (López-Sánchez et al., 2005; Lorent et al., 1995) when upper layer neurons are generated (Molyneaux et al., 2007). In order to visualize electroporated cells, EGFP was coexpressed. As control, we used a scrambled control shRNA that does not align significantly with any NCBI mouse transcript sequence. Four days after electroporation, the time point when transfected precursors are expected to have differentiated into neurons which are residing in the upper layers of the cortical plate (Fig. 1B), we fixed the brains and analysed the position of labelled cells in coronal sections. For this purpose we divided the cortex into ten equal bins and counted the relative number of EGFP-positive cells in each bin (see Materials and Methods; Fig. 1B,C). Moreover, we analysed the difference of the entire population distribution (Fig. 1C, inset). Both types of analysis did not reveal any difference in the behaviour of APLP2 shRNA expressing cells in respect to control shRNA cells (Fig. 1B,C). In both cases, EGFP-positive cells were mostly positioned in the upper layers of the cortex, which is marked by Cux1 antibody (Fig. 1B).

We considered the possibility that the well-described redundant function of APP, APLP1 and APLP2 throughout development (Heber et al., 2000) could have led to a compensation for the loss of APLP2 function. To test this, we expressed APLP2 shRNA in cortical progenitors from APP/APLP1 dko mice. APLP2 downregulation in APP/APLP1 dko resulted in a large number of EGFP-positive cells (54%) residing in the Cux1 negative region, i.e. predominantly in the VZ/SVZ of the developing cortex (Fig. 1D,E). Similar to wt mice, the majority of neurons electroporated with the control shRNA construct (APP/APLP1 dko) migrated to the upper layer of the cortical plate (Cux1-positive layer, Fig. 1D). This indicates that APLP2 is an important component of the machinery responsible for proper neuronal progression towards the cortical plate. To guard against possible off-target of the APLP2 shRNA construct, we used a second shRNA (i.e. shRNA2) to target APLP2 in the developing cortex. Again, we find only a change in the cortical positioning of cells transfected with APLP2 shRNA2 in APP/APLP1 dko mice (supplementary material Fig. S1). Moreover, the inability of both APLP2 shRNA constructs to induce any phenotype in wt cortices (Fig. 1B,C; supplementary material Fig. S1) argues for the specificity of our approach.

Next, we asked whether the morphology of neurons that are moving towards the cortical plate is different in dko versus 'triple ko' neurons, which could explain the observed changes in cortical positioning of the cells. Careful microscopic analysis revealed that this is not the case: neurons in both groups displayed the typical bipolar morphology of migrating neurons with a thickened leading edge and a thinner trailing process (Fig. 2A), indicating that APLP2 is not essential for the acquisition of the morphological polarization required for proper migration. To assess directly neuronal migration, we monitored the migration speed and distance of dko neurons either expressing the control shRNA or the APLP2 shRNA through the use of an *in vitro* migration assay in Matrigel (Calderon de Anda et al., 2008). We did not detect any differences in the distance that double or 'triple' ko neurons migrate away from the explants (Fig. 2B). Moreover, live imaging of migrating neurons did not reveal differences in the speed of neuronal migration nor in the morphology nor in the behaviour of the migrating neurons (Fig. 2B; supplementary material Movies 1 and 2). Thus, neither a morphological defect nor the migratory behaviour of neurons is the cause of altered cortical positioning.

To test whether the migration delay was due to a change in the morphological differentiation of radial glia cells, which provide the scaffold for radially migrating neurons, we analysed the morphology of EGFP-labelled radial glia cells in E16.5 dko slices of mice with downregulated APLP2 from E14.5. The morphology of radial glia was similar in APLP2 shRNA and control plasmid electroporated dko cortices: they were radially oriented, well aligned and spanned the entire cortical wall with branched basal end feet and apical connections (Fig. 2C) (Chanas-Sacre et al., 2000).

'Triple knockout' cells remain in a proliferative progenitor state

Apart from the defective cortical positioning of 'triple knockout' neurons described above, we also detected retention of 'triple knockout' cells in the VZ/SVZ (Fig. 1D,E). To determine whether the cells arrested in the VZ/SVZ are progenitors which remain longer in a proliferative state, or neurons which fail to migrate away from the proliferative zones, we labelled the brain slices with the basal progenitor marker Tbr2 (Fig. 2D). In dko cortices electroporated with the control shRNA a small number of EGFP positive cells were located in the VZ/SVZ and only 7% ($\pm$s.d. 2.4%, $n=3$) were Tbr2 positive, demonstrating that four days after electroporation, most of the cells became post-mitotic and migrated to the cortical plate (Fig. 2D). In contrast, in dko cortices electroporated with the APLP2 shRNA, a large number of cells remained in the VZ/SVZ of which 29% ($\pm$s.d. 3.5%, $n=3$) expressed Tbr2 suggesting that they failed to differentiate into post-mitotic neurons (Fig. 2D). In addition, a Tbr2 negative population in the ventricular zone, most likely radial glia progenitors (see later), was still present (Fig. 2D,E) and some cells (Fig. 2E) were still expressing phospho-histone 3 (PH3), a marker tightly associated to chromosome condensation during mitosis (Goto et al., 1999), showing that they were undergoing mitosis. In contrast, in dko cortices electroporated with the control shRNA we very rarely found mitotic PH3/EGFP-positive cells and only observed a very small number of radial glia cell progenitors.

Altogether, these data suggest that APLP2 plays a role in the normal progression of the neuronal differentiation program from precursors to post-mitotic neurons.

APLP2 has a progenitor-specific function and is dispensable for radial migration

To substantiate the above hypothesis, we designed a construct to achieve cell-specific expression of the APLP2 shRNA, based on the use of a let-7 microRNA embedded shRNA that can be expressed from cell-type-specific promoters (Fig. 3A). The let-7 microRNA based shRNA was more effective in downregulation of mCherry compared to the commonly used miR-30 microRNA system (data not shown). Its functionality for APLP2 downregulation was proven by western blot analysis of

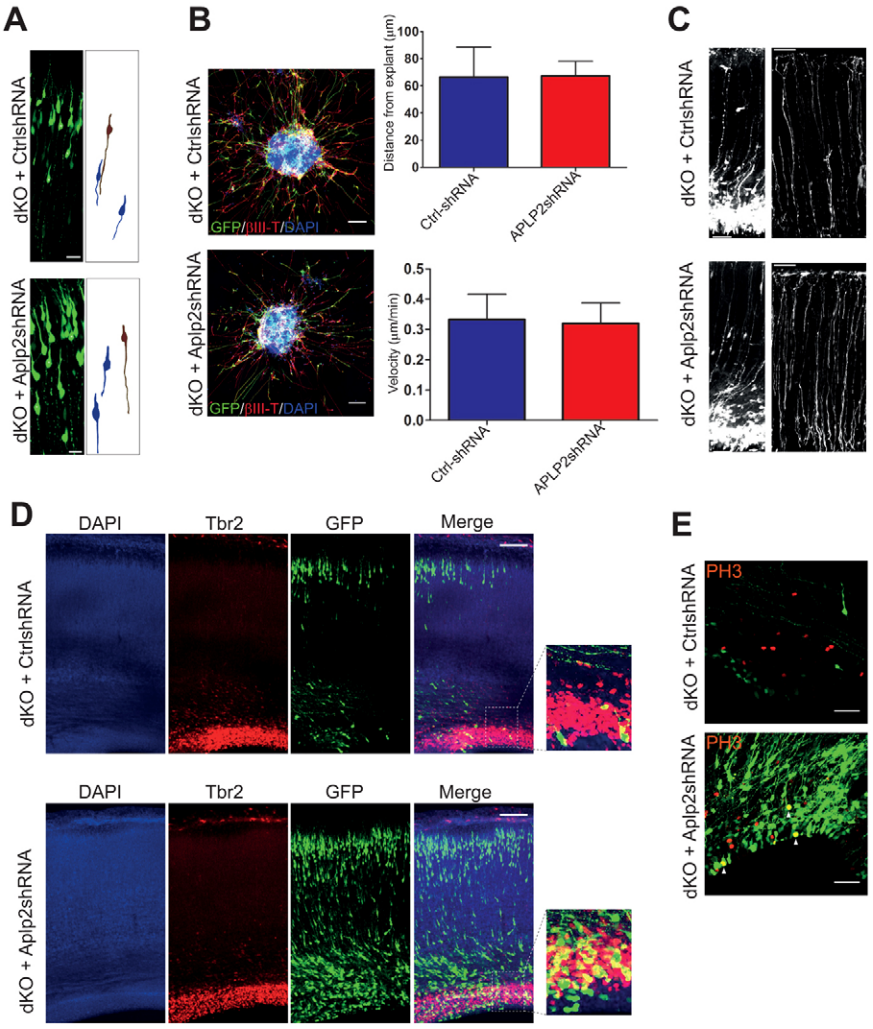

Fig. 2. Arrested 'triple ko' cells express progenitor and mitotic markers but do not show morphological changes. (**A**) Confocal images of 20–25 (0.8 μm) consecutive *z*-sections illustrating morphology of dko migrating neurons transfected with APLP2 shRNA or control shRNA. Drawings on the right depict the morphology of two migrating neurons (blue) and one positioned in the CP. The morphology of neurons in both groups is comparable. (**B**) Images of control shRNA or APLP2 shRNA transfected neuronal explants embedded in Matrigel 3 days after plating. The upper graph shows the mean distance of EGFP-positive cells from the margin of explants, which does not change in triple ko neurons. Values represent the mean ± s.d. (n=3 different experiments, control, 161 cells from 16 explants; shRNA, 182 cells from 18 explants; Student's t-test). The lower graph shows that the velocity of neuronal movement does not change with expression of APLP2 shRNA (n=2 independent experiments, 29 cells for APLP2 shRNA and 26 cells for control shRNA). (**C**) Confocal projection images of 20–25 consecutive *z*-sections (0.8 μm) of radial glia cells illustrating their ascending fibres (left) and end feet (right) in APP/APLP1 dko cortices transfected with APLP2 shRNA or control shRNA. In both groups, the fibres span the entire cortical wall with branched end feet that are attached to the pial surface. (**D**) APP/APLP1 dko cortices transfected with APLP2 shRNA or control shRNA construct coexpressing EGFP. Confocal images of coronal cortical sections labelled with Tbr2 antibody 4 days after electroporation show progenitors in the VZ/SVZ of APLP2 shRNA-treated cortices. (**E**) APP/APLP1 dko cortices transfected with APLP2 shRNA or control shRNA labelled with the mitotic PH3 marker show mitotic APLP2 shRNA transfected cells (white arrowheads). Scale bars: 25 μm (A, C right); 50 μm (B, C left, E); 100 μm (D).

HEK293 cells expressing a V5 tagged APLP2 cDNA and transfected with a shRNAmir construct (Fig. 3B). Similar to the U6-APLP2 shRNA constructs (Fig. 1A), the APLP2 shRNAmir construct reduced APLP2 protein expression by about 90%. Moreover, E14 cortical cultures transfected with APLP2 shRNAmir, showed comparable downregulation of endogenous APLP2 to the U6-driven shRNA (supplementary material Fig. S2A). In addition, *in utero* electroporation of APLP2 shRNAmir using the ubiquitous CAG promoter recapitulated the phenotype (supplementary material Fig. S2B) that was obtained by the U6 driven APLP2 downregulation in dko mice (Fig. 1D).

This system allowed us to investigate the result of a cell specific loss of APLP2 function by driving the expression of APLP2 shRNA in neural progenitors and post-mitotic neurons using the Brain lipid-binding protein (BLBP) and Tubulin-α (Tα) promoters, respectively (Coksaygan et al., 2006; Feng et al., 1994; Gloster et al., 1994; Hashimoto-Torii et al., 2008). Differential expression of Tα and BLBP promoters was confirmed by co-electroporation of Tα-mCherry with BLBP-EGFP *in utero* (Fig. 3C).

Expression of APLP2 shRNAmir under the control of neuronal Tα promoter in dko post-mitotic cells did not result in any changes in the cortical positioning of EGFP-positive cells when compared with control shRNA (Fig. 3D,E). In contrast, progenitor specific expression of APLP2 shRNAmir caused the accumulation of cells in the VZ/SVZ similar to the phenotype that we observed using the U6 promoter (compare Fig. 3F,G with Fig. 1D,E). In order to visualize the progeny of cells electroporated with BLBP APLP2 shRNAmir after the BLBP promoter is switched off in young neurons, we co-electroporated a mCherry-expressing construct with the ubiquitous CAG promoter. Four days after electroporation we detected BLBP-EGFP-positive cells only in the APLP2 shRNAmir expressing cortices (Fig. 3F). This supports a progenitor specific function of APLP2 and the delay in the exit from the progenitor stage, further highlighting the importance of APLP2 in neural differentiation of cortical progenitors.

Cell cycle variables are regulated by APLP2

In order to understand the role of APLP2 during precursor proliferation in more detail, we chose to analyse *in utero* electroporated brains two days after electroporation instead of four days. After two days, a substantial number of progenitors can still be found in the proliferative zone of the developing cortex even under control conditions (Tabata and Nakajima, 2001; Tabata and Nakajima, 2008), allowing us to compare the proliferative fraction of cells under different conditions, whilst after 4 days most of the progeny deriving from *in utero*

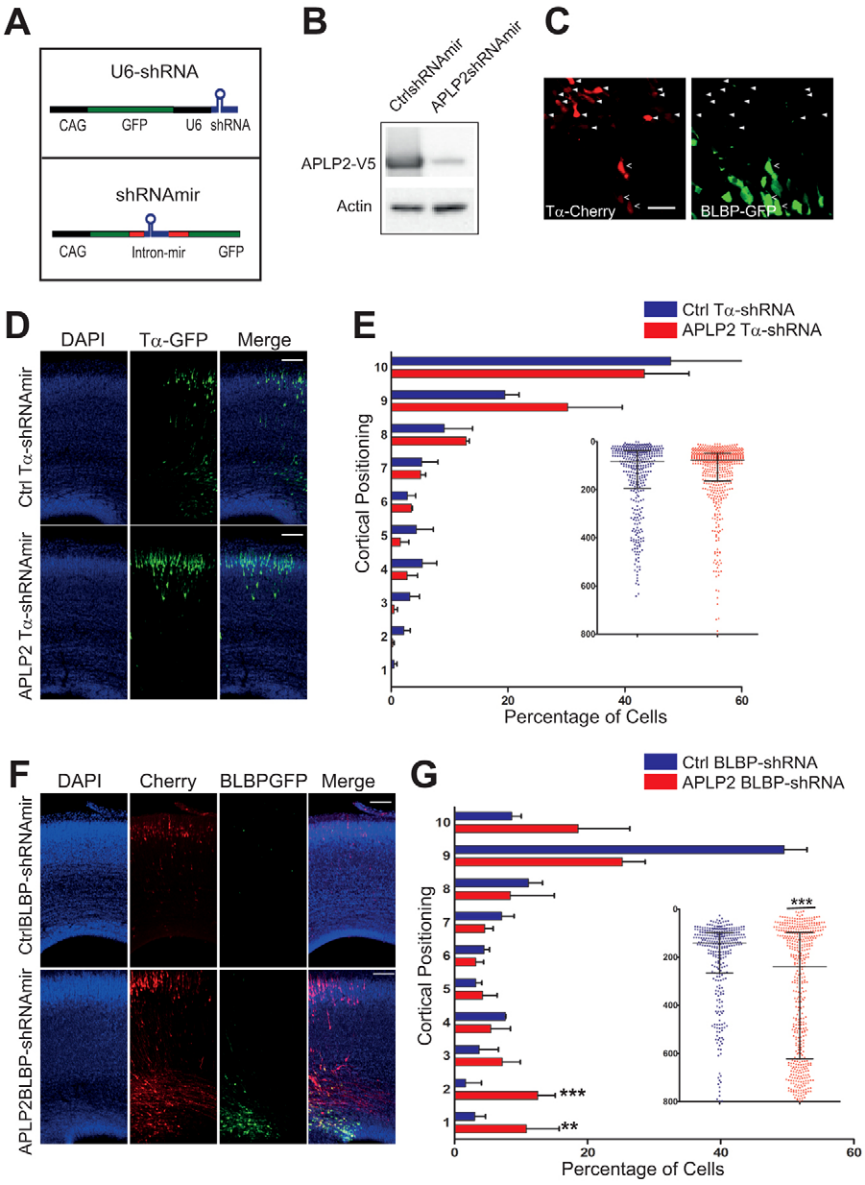

Fig. 3. Progenitor-specific expression of APLP2 shRNA is sufficient to retain cells in the proliferative zone of developing cortex. (**A**) Schematic comparison of U6-shRNA and microRNA-based shRNA. (**B**) Western blot showing protein levels of APLP2-V5 and actin (loading control) of HEK cells expressing APLP2-V5 transfected with APLP2 shRNAmir or control shRNAmir. The downregulation obtained by the microRNA construct was about 90% and comparable to the efficiency of the U6 shRNA1 construct (see Fig. 1A). (**C**) Co-transfection of Tα-cherry (solid arrowheads) with BLBP-GFP using *in utero* electroporation (E14.5–E16.5) shows that the two promoters target different cell populations because only a very small fraction of cells coexpress mCherry and EGFP (6.12%; 150 cells, open arrowheads). (**D**) Confocal images (projection of 10–15 consecutive *z*-sections) of dko cortical slices transfected with APLP2 shRNAmir or control shRNAmir under the control of Tα promoter. Neuronal downregulation of APLP2 does not change cortical positioning. (**E**) Quantification of EGFP-positive cells shown in D. Bar graphs represent frequency distribution of EGFP-positive cells in ten equally divided bins from ventricle (1) to the pial surface (10) of the cortical wall. Values represent the mean ± s.d. (n=3; Student's t-test). The inset scatter plot compares the population distribution of EGFP-positive cells (n=3, 300–400 cells for clarity of graph; values represent the median ± interquartile range, Mann–Whitney test). (**F**) Confocal images (projection of 10–15 consecutive *z*-sections) of dko cortical slices transfected with APLP2 shRNAmir or control shRNAmir under the control of BLBP promoter. Progenitor-specific expression of shRNA leads to retention of cells in the VZ/SVZ. (**G**) Quantification of Cherry-positive cells shown in F. Bar graphs represent the frequency distribution of Cherry-positive cells in ten equally divided bins from ventricle (1) to the pial surface (10) of the cortical wall. Values represent the mean ± s.d. (n=3; Student's t-test). The inset scatter plot compares the population distribution of Cherry-positive cells (n=3, 300–400 cells; values represent the median ± interquartile range, Mann–Whitney test). $^{**}P<0.01$, $^{***}P<0.001$. Scale bars: 50 μm (C); 100 μm (D,F).

electroporated progenitors has been differentiated into neurons (Fig. 1D,E).

Initially, we analysed the position of APLP2 shRNAmir expressing cells and found a higher number of cells compared to control transfected cells many of which were located closer to the ventricle (Fig. 4A). This initial observation suggested that APLP2 may be involved in the regulation of progenitor proliferation. Alternatively, the higher number of cells simply reflects differences in electroporation efficiencies. To distinguish between these possibilities, we analysed the fraction of EGFP positive cells which were still proliferating under control and 'triple ko' conditions. To determine which fraction of the progenitor pool remains in the proliferative state, we examined cell cycle exit rates of EGFP-positive cells after *in utero* electroporation of E14 cortices and BrdU (5-bromo-2′-deoxyuridine) pulse labelling of S-phase cells 24 hours before collecting the brains at E16.5. This was followed by Ki67 staining, which is expressed throughout the cell cycle and thus labels all proliferating cells (Chenn and Walsh, 2002). Hence, the cells which integrate BrdU and express Ki67 after 24 hours correspond to the proliferative pool, while Ki67 negative but BrdU positive cells correspond to the pool of cells that have recently exited mitosis, and consequently are young neurons. The rate of cell cycle exit was calculated as the ratio between EGFP+/BrdU+/Ki67− cells and the total EGFP+/BrdU+ population. This ratio was significantly decreased from 74% in ctrl shRNAmir expressing cells to 45% in APLP2 shRNAmir dko cells, demonstrating essential function of APLP2 in the regulation of neuronal differentiation (Fig. 4B). In light of these findings, the observed decrease in neuronal progression and resulting changes in cortical positioning of 'triple ko' cells likely results from delay in the cell cycle exit rate and a delayed entry into the neuronal differentiation program.

We reasoned that a reduced cell cycle exit rate can result in more mitotic cells in 'triple ko' conditions. To test this hypothesis, we labelled specifically mitotic cells using an antibody against phosphorylated histone 3 (Ser10). Two days after electroporation a twofold increase in the number of mitotic

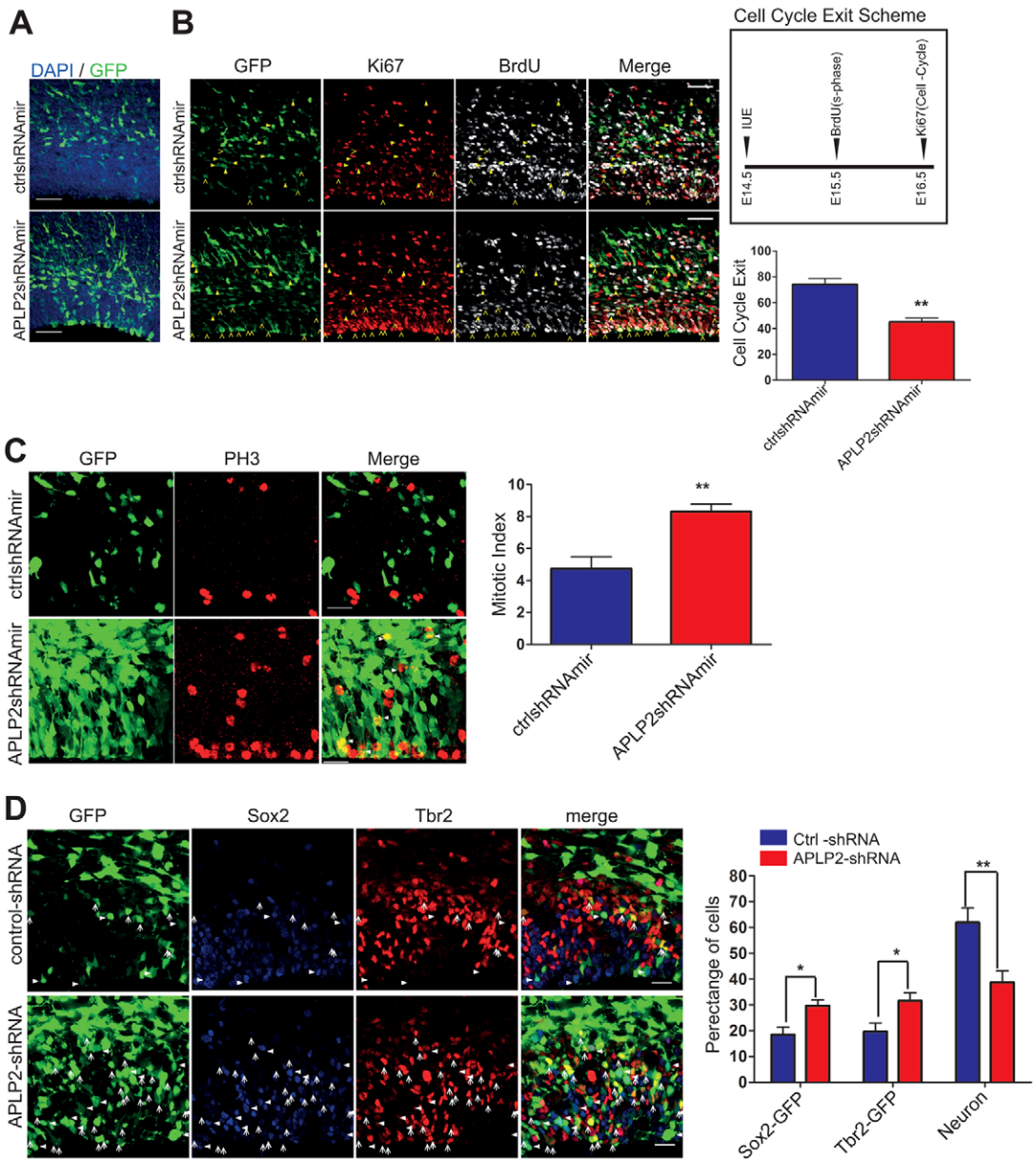

Fig. 4. Downregulation of APLP2 leads to decreased cell cycle exit and expansion of progenitor pools. (**A**) Confocal images (projection of 10–15 consecutive *z*-sections) of E16 dko cortical slices co-transfected with APLP2 shRNAmir or control shRNAmir at E14. Two days after electroporation, more cells are found close to the VZ of the developing cortex in APLP2 shRNA expressing cortices. (**B**) Confocal images of dko cortices transfected by APLP2 or control shRNA at E14.5 followed by BrdU injection at E15.5 and then triple staining for EGFP, BrdU and Ki67 at E16.5 (see scheme of the cell cycle exit assay). Open yellow arrowheads indicate the cells that did not leave the cell cycle; solid yellow arrowheads indicate EGFP+/BrdU+/Ki67− cells. The graph shows the decreased cycle exit of APLP2 shRNA-expressing progenitors that is calculated by the ratio of EGFP+/BrdU+/Ki67− cells divided by the total EGFP+/BrdU+ population (n=5). (**C**) Confocal images as in B, labelled with the mitotic PH3 marker. After APLP2 downregulation the number of mitotic cells increased (white arrowheads). Graph shows mitotic index as calculated by the ratio of PH3+ cells divided by the total number of EGFP-positive cells. Values represent the mean ± s.d. (n=3). (**D**) Confocal images of Sox2-Tbr2 double-stained slices transfected with APLP2 shRNA or control shRNA. Solid white arrowheads indicate EGFP/Sox2 double-positive progenitors; white arrows indicate EGFP/Tbr2 double-positive progenitors. The graph shows that both classes of progenitors are increased after APLP2 downregulation (n=3). Values represent the mean ± s.d.; *P<0.05, **P<0.01, Student's t-test. Scale bars: 50 µm (A); 100 µm (B); 25 µm (C); 20 µm (D).

cells was observed in VZ/SVZ of dko cortices electroporated with APLP2 shRNAmir when compared to control shRNAmir (Fig. 4C).

The observed changes in progenitor proliferation raised the question of whether this had resulted in a different distribution of the progenitor and neuronal pools. The balance between progenitors and post-mitotic neurons depends on the ratio of neurogenic versus proliferative radial glia cell division. A proliferative division can be self-renewing or leading to the generation of a radial glia cell and intermediate progenitor cells. These two principal classes of progenitors can be distinguished by specific molecular markers: Sox2 for radial glia and Tbr2 for intermediate progenitor cells. We therefore used double-staining of Sox2 and Tbr2 to determine the balance between proliferative

and neurogenic division of radial glia cells after APLP2 downregulation. APLP2 downregulation in dko cortices significantly increased both Sox2 and Tbr2 EGFP-positive cells with a corresponding relative paucity of post-mitotic neurons (Fig. 4D). This result shows that lack of APLP2 shifts radial glia cells towards proliferative division, implying that APLP2 is involved in neurogenic division.

Discussion

Our data are consistent with the view that APLP2 plays a key role in the essential biological decision of differentiating a neuronal progenitor into a neuron. The control of this step is essential during cortical development since there is a close link between the timing of the cell cycle exit and the determination of the laminar fate of the generated neurons (McConnell and Kaznowski, 1991). Hence, prospective cortical architecture is already determined at early developmental stages.

Previously, we analysed neurons generated *in vitro* from triple ko APP/APLP1/APLP2 embryonic stem cells (Bergmans et al., 2010) and did not find any obvious phenotype. This prompted us to further investigate the role of APP gene family *in vivo*. Among the different combinatorial genetic deletions of APP/APLPs in mice, only APP/APLP1 double ko is a viable genotype, suggesting a crucial and distinct developmental role for APLP2 (Heber et al., 2000). Therefore, in order to study APLP2 function and to preclude redundancy, we analysed the role of APLP2 in APP/APLP1 dko mice. In order to avoid lethality, we downregulated APLP2 in a subpopulation of cells in the ventral telencephalon by *in utero* electroporation of shRNA against APLP2 (Fig. 1). The cells are indeed viable under those conditions as shown by their even increased proliferation rate and their normal morphology (Figs 2, 4). Although our studies demonstrate that APLP2 downregulation alone is not sufficient to elicit developmental defects (Fig. 1B,C), a number of indications reveals a central role of APLP2: APLP2 is specifically distributed in the proliferative VZ and SVZ of the developing cortex. In contrast, APLP1 is restricted to the CP where differentiated neurons reside and APP is present rather non-specifically in the VZ/SVZ and CP (López-Sánchez et al., 2005). Thus, APP residing in the VZ/SVZ could be responsible for the redundant effect on proliferation.

We show that reduced level of APLP2 in APP/APLP1 dko progenitors led to decrease of cell cycle exit and preservation of progenitors in their proliferative stage (Fig. 4B,D). APLP2 is a trans-membrane protein with a large extracellular multidomain region and could therefore regulate the proliferation of progenitors in various ways. The extracellular domain could be involved in receptor–ligand or in cell-adhesion interactions. The intracellular domain, which contains a YENPTY motif can bind several adapter molecules some of which are involved in the control of neurogenesis such as Dab1 (Homayouni et al., 1999; Lakomá et al., 2011), Numb (Roncarati et al., 2002) and Fe65 (Ma et al., 2008). Numb is involved in cell fate decisions such as proliferation versus differentiation by its repressing activity on Notch (Roncarati et al., 2002). Active Notch is promoting the self-renewal of specifically radial glia progenitors (Yoon et al., 2004), the population which is also increased after APLP2 downregulation in progenitors of dko mouse (Fig. 3F; Fig. 4D). Interestingly, Thr^{668} close to the APLP2 YENPTY interaction domain can be phosphorylated by a CDK1 kinase changing the binding properties of the YENPTY motif and thus couples APLP2 function and metabolism to the cell cycle (Suzuki et al., 1997; Tamayev et al., 2009). Similar to APLP2, CDK1 expression is also concentrated in the VZ/SVZ of developing cortex (Diez-Roux et al., 2011; Visel et al., 2004) suggesting that CDK1 could be involved in the regulation of neuronal development through APLP2. Alternatively, APLP2 which plays a role in cell–cell and cell–extracellular matrix interactions (Müller and Zheng, 2012; Soba et al., 2005) could directly regulate the decision between progenitor proliferation and differentiation into neurons, which is strongly dependent on specific membrane associated factors (Temple and Davis, 1994). Indeed, at the neuromuscular junction, APP family proteins are proposed as novel synaptic adhesion molecules (Wang et al., 2009) and it will be of interest to investigate a similar role in the context of neuronal progenitor differentiation. An analysis of proteins interacting specifically with APLP2 revealed members of the RhoGTPase family such as Rac1 and RhoA (Bai et al., 2008), which can potentially influence cell cycle progression (Vidaki et al., 2012; Yang et al., 2012). A recent DNA microarray transcriptome profiling of the adult prefrontal cortex showed that the expression of genes involved in neurogenesis is altered in APLP2 ko brains (Aydin et al., 2011). In this study, CDK inhibitor p21 was found to be downregulated in APLP2 ko mice. Downregulation of p21 enhances progenitor proliferation in the adult hippocampus (Pechnick et al., 2008). It will be interesting to determine whether similar mechanisms are relevant for embryonic neurogenesis regulation.

In order to investigate which progenitor populations were affected after APLP2 downregulation, we analysed the proportion of radial glia (Sox2 positive) and intermediate (Tbr2 positive) progenitors in cells two days after ubiquitous APLP2 downregulation (Fig. 4D). We observed not only an expansion of the radial glia cell pool, but also that of intermediate progenitors (Fig. 4D), which mainly divide symmetrically into neurons (Haubensak et al., 2004). Interestingly, many Tbr2 positive intermediate progenitors were found in the VZ indicating that they were generated recently by radial glia cells (Fig. 4D). This suggests that their increase is a consequence of the larger pool of radial glia cells which are generating more intermediate progenitors. Our data do not support, but cannot completely exclude, a direct influence of APLP2 on intermediate progenitor division and/or migration.

Our studies showed that APLPs and APP appeared largely dispensable for the radial migration of cortical excitatory neurons. Cortical neuron positioning in APP/APLP1 double knockout mice or in APLP2 knockdown cells was indistinguishable from that in wild-type mice (Fig. 1B–E). We found differences in cortical positioning in ‘triple ko’ mice (Fig. 1D,E). This delay in cortical neuron progression towards the CP is likely a consequence of a primary defect in progenitor function: first, we could not detect any differences in migration speed of isolated ‘triple ko’ neurons and wt neurons using an *in vitro* assay (Fig. 2D); second, we could phenocopy the accumulation of cells close to the VZ/SVZ by expressing APLP2 shRNA only in progenitors of dko mice (Fig. 3E,F). The absence of a migration defect contrasts with other findings showing abnormalities in neuronal migration during cortical development. Yet, the findings of these studies were not conclusive, one study showing a complete inhibition of cortical plate entry and the other an ectopic accumulation of neurons in the marginal zone (Heber et al., 2000; Young-Pearse et al., 2007).

However, these studies did not investigate progenitor function which could be a possible alternative or additional explanation for the observed cortical positioning defects. Taken together, the current data support a model in which APP is functional in both progenitors and post-mitotic migrating neurons, whilst APLP2 is playing a specific role in regulating progenitor proliferation and differentiation.

In summary our data contribute to our understanding of the contribution of the APP family molecule APLP2 in the early developmental steps of the cerebral cortex, which lays the basis for subsequent development of correct cortical networks.

Materials and Methods

DNA constructs

The APLP2 shRNA1 (GI562807) (sequence: 5′-CGATTACAATGAGGAGAATCCAACCGAAC-3′), the APLP2 shRNA2 (GI562808) (sequence 5′-ATGAAGGCTCTGGAATGGCAGAACAAGAC-3′) and control shRNA (scrambled sequence: 5′-GCACTACCAGAGCTAACTCAGATAGTACT-3′) driven by the U6 promoter were obtained from Origene (Rockville, MD).

The *pCAG-EGFPintron-let-7f*-based shRNA expression system was constructed as follows. The synthetic intron found in the psicheck2 plasmid (Promega, Leiden, The Netherlands) was PCR amplified using Promega IntronF (5′-CGAAGGTAAGTATCAAGGTTACAAGACAG-3′) and R (5′-GACGTAGCCTGTGGAGAGAAAGGCAAAGTG-3′) primers. The intron was then inserted into EGFP by overlap-PCR using two inner primers for 5′ (5′-TGATACTTACCTTCGGGCATGGCGGACTTGAAG-3′) and 3′arms (5′-TCTCTCCACAGGCTACGTCCAGGAGCGCACCATCTTCTTC-3′) of EGFP and two outer primers for 5′ (5′-GCCACCGGTCGATCCACGCCACCATGGTGAGCAAGGGCGAGGAG-3′) and 3′ (5′-GATTGTCGACTTACTTGTACAGCTCGTCCATGCCG-3′) arms. Next, *Xho*I and *Eco*RI restriction sites were added to the intron by PCR using Intron *Xho*I-*Eco*RI-F (5′-GAATTCCAATCTCGAGCTATTGGTCTTACTGACATCCACTTTGC-3′) and Intron *Xho*I-*Eco*RI-R (5′-CTCGAGATTGGAATTCAGCCTATCAGAAACGCAAGAGTCTTCTCTG-3′) primers (pCAG-EGFP intron). The let-7f2 genomic sequence was amplified from human genomic DNA using LET-7Fhu-MfeI (5′-TCATCAATTGTAACTCTCCTTCCCTTTCTCCCTTCTTAC-3′) and LET-7Fhu-*Sal*I (5′-TCATGTCGACCATCAAAGGACCAGCCACTT-3′) primers and cloned into the pCAG-EGFP intron vector digested by *Xho*I and *Eco*RI. This intermediate construct contains the genomic sequence of human let-7f2 precursor including the mature let-7f sequence. In order to remove this mature sequence and facilitate cloning of shRNAs, the 5′ and 3′ arms of the let-7f scaffold were amplified using two inner primers: 5′ arm (5′-GGCGCGCCCTCGAGCCATCTTCAGCCTATGTGGG-3′) and 3′ arm (5′-GGCGCGCCG AATTCTCTTCTCCGACTGGCTCTGTTC-3′) scaffold and two outer primers: Let7F-XhoI (5′-CAATCTCGAGGTGCTCTGTGGGAT-3′) and Let7F-*Eco*RI (5′-CAATGAATTCGTACCACCGTGGGA-3′). The PCR product was cloned into the intermediate construct resulting in the pCAG-EGFPintron-let-7f plasmid. For shRNA cloning, overlapping DNA oligonucleotides were designed to embed the shRNA into the let-7f scaffold sequence. The shRNAs for APLP2 and mCherry were obtained after annealing the following oligonucleotides: APLP2-let7-I (5′-CTCGAGGTGCTCTGTGGGATCGCTGCTGGGTTCGGTTGGATTTAGGGTCATACCCCATCTTG-3′); APLP2-let7-II (5′-GAATTCGTACCACCGTGGGACGCCACTGGGTTCGGTTGGATATCTCCAAGATGGGGTATGAC-3′); mCherry-let7-I (5′-CTCGAGGTGCTCTGTGGGATGATGTTGACGTTGTAGGCGCCTTAGGGTCATACCCCATCTTG-3′); mCherry-Let7-II (5′-GAATTCGTACCACCGTGGGAGATACTGACGTTGTAGGCGCCATCTCCAAGATGGGGTATGAC-3′) and PCR amplified using pre-Let7F and pre-Let7R universal primers. The resulting shRNAs were digested and cloned into the pCAG-EGFPintron-let-7f plasmid using *Xho*I and *Eco*RI restriction sites.

BLBP-shRNA mir

For cell-specific expression into radial glia cells, the BLBP promoter was amplified from mouse genomic DNA using BLBP-F (5′-CAATGTCGACAGCACAGCAGAAAGGGAAAA-3′) and BLBP-R (5′-GGTGGGCGCGCCAGGCAGGAACTGGAGGAACTC-3′) primers and cloned into the pCAG-EGFPintron-let-7f digested by *Sal*I and *Asc*I, thus replacing the CAG promoter by the mouse BLBP promoter.

Tα-shRNAmir

The tubulin alpha promoter was chosen to drive neuronal expression and amplified from mouse genomic DNA using Tα-F (5′-ACCTACTAGTGTATTAGAAGGGATGGCTCA-3′) and Tα-R (5′-ACCTACCGGTGGTTGCTGCTTCGCGGCTGCC-3′) primers and cloned into the pCAG-EGFPintron-let-7f digested by *Spe*I and *Asc*I. For *in utero* electroporation, DNA preparations, included endotoxin removal treatment, were obtained using Qiagen EndoFree Plasmid Maxi Kit (Qiagen, Venlo, The Nethelands), with final concentration between 2 and 3 μg/μl plasmid DNA.

Western blot

Total cell lysates of cortical neuron cultures or HEK293 were prepared in cell lysate buffer (1% Triton-X100, with protease inhibitors in PBS). 20 μg of protein was separated on a NuPAGE 4–12% (Invitrogen), transferred to nitrocellulose and membranes were incubated overnight at 4℃ with the following primary antibodies: APLP2 (CT12 a kind gift from G. Thinakaran, University of Chicago, IL), V5 antibody (1:10,000-mouse, Invitrogen Gent, Belgium), APP antibody (B63-1:5000, custom made rabbit antibody), GAPDH (1:5000-mouse, HyTest), Actin (1:1000-mouse, Sigma-Aldrich, Diegem, Belgium) and detected with HRP conjugated secondary antibodies using a ECL chemiluminescence detection kit (PerkinElmer Life Sciences, Zaventem, Belgium). The density of bands was quantified by densitometry using Aida Image Analyser 4.27 (Raytest, Straubenhardt, Germany) and linearity of the signal was tested using different dilution of total cell lysate.

Cell cultures

Mouse embryonic cortical neurons were prepared as described previously (Banker and Goslin, 1988) and plated at a density of 100,000 cells/cm^2 on poly-L-lysine (PLL) coated dishes. Neurons were transfected before plating using nucleofection (Amaxa, Cologne, Germany). HEK293 cells overexpressing V5 tagged APLP2 were grown in DMEM/F12 with 10% fetal calf serum (FCS) and were transfected with shRNA expressing construct using TransIT®-LT1 transfection reagent (Mirus, Madison, WI).

Matrigel assay for migration

E14 embryonic cortices were dissected and digested by papain for 20 minutes at 37℃. After subsequent mechanical dissociation, cells were transfected by nucleofection (Amaxa) followed by overnight shaking (350 rpm) at 37℃ to form aggregates. The aggregates were embedded in Matrigel (BD Biosciences, Erembodegem, Belgium) on coverslips and fixed in 4% paraformaldehyde (PFA) after 3–4 days. For live imaging from one day after plating onwards, coverslips were mounted in a closed metal chamber and images were acquired at 20 minutes intervals for up to 24 hours using an inverted Olympus Cell^R microscope.

Transgenic mice

APP/APLP1 double knockout mice were described previously and generated by genomic deletion of the promoter and initiation codon of APP and APLP1 loci (Heber et al., 2000; Herms et al., 2004). Wild-type embryos were from C57/Bl6 background.

In utero electroporation

All animal experiments were approved by the Ethics Committee of the K.U. Leuven. Pregnant mice were anaesthetized by intramuscular injections of 88 μg ketamine and 132 μg xylazine per gram of body weight. The uterine horns were exposed and the plasmids (1–2 μg/μl) mixed with Fast Green (Sigma) were microinjected in the lateral ventricles of E14.5 mouse embryos. Five current pulses (50 milliseconds pulse/950 milliseconds interval) were delivered across the head of the embryos (36 V) targeting the dorsal-medial part of the cortex. After 2–4 days, embryos were collected and perfused with PBS and 4% PFA and the brains postfixed for 6–10 hours in 4% PFA at 4℃.

Immunocytochemistry

Coronal vibratome sections of the fixed embryonic brains were prepared with 100 μm thickness. Subsequently, the sections were permeabilized and blocked at RT for 1 hour in PBS, 0.3% Triton X-100, 3% BSA, 5% goat or donkey normal serum, incubated with the primary antibody at 4℃ overnight followed by the secondary Alexa-Fluor-conjugated antibodies for 2 hours at room temperature (Invitrogen). For BrdU detection, slices were pre-treated with 1 M HCl (10 minutes 4℃) and 2 M HCl (10 minutes RT and 20 minutes 37℃) with subsequent washes in 0.1 M borate buffer.

The following primary antibodies were used: chicken anti-EGFP (1:500; Aves Labs, Oregon), rabbit anti-Ki67 (1:300; Novacastra, Diegem, Belgium), rabbit anti-Tbr2 (1:1000; Abcam, Cambridge, UK), rabbit anti-PH3 (1:300; Cell Signaling, Leiden, The Netherlands), rabbit anti-βIII-tubulin (1:1000, Abcam), mouse anti-BrdU (1:200; Roche, Vilvoorde, Belgium), rabbit anti-Cux1 (1:500; Santa-Cruz, Heidelberg, Germany), goat anti-Sox2 (1:150; Santa-Cruz). Nuclei were visualized with DAPI.

Cell cycle exit

One day after *in utero* electroporation, pregnant mice were injected intraperitoneally with BrdU (75 mg/kg, Sigma-Aldrich). After another 24 hours the brains were collected, fixed and immuno-stained using anti-EGFP, anti-BrdU

and anti-Ki67 antibodies. The cell cycle exit rate was calculated as the ratio of $EGFP^+/BrdU^+/Ki67^-$ cells (cells which are not in the cell cycle) divided by the number of $EGFP^+/BrdU^+$ cells (total number of dividing and non-dividing cells).

Confocal imaging and quantification

Confocal images were captured on a Nikon microscope (Eclipse; Ti A1) using an Apo 10× 1.40 N.A. objective lens. The images were acquired by Nis-Element software and the imaging parameters were kept constant during imaging. Ten to fifteen consecutive *z*-sections were obtained per brain slice. All images were processed using the ImageJ software (NIH).

For cortical positioning

The entire length of cortical walls was divided into ten equal bins and the frequency of cells per bin was calculated by counting the cell bodies of EGFP-positive cells in each bin, divided by the total number of EGFP-positive cells.

For cell cycle exit

All the images were thresholded and BrdU+/EGFP+ cells were detected by the AND function of Image Calculator (ImageJ software). Next, the same function was used to find BrdU/EGFP double positive cells that are positive or negative for Ki67.

Statistics

Corresponding bins were compared using Student's *t*-test. The population distribution of two groups of neurons was compared using a non-parametric Mann–Whitney U test ($P<0.05$ as significance level). All statistical analysis and graph preparation were performed by using GraphPad Prism5.

Acknowledgements

We wish to thank T. Wahle, T. Achsel, P. Fazzari, B. Bergmans, L. Serneels, and A. Thathiah from our institute for their critical feedback on the project; G. Thinakaran (University of Chicago, IL) for providing us with the CT12-APLP2 antibody; and V. Hendrickx, J. Verwaeren and G. Mariën for their great technical assistance with mice.

Author contributions

S.A.M.S., B.A.H., B.D.S., C.D. and A.G. designed the project; S.A.M.S., P.L. and A.G. performed research, U.M. contributed reagents, S.A.M.S. and A.G. analyzed the data and S.A.M.S., B.D.S., C.D. and A.G. wrote the paper.

Funding

This work was made possible by grants from the Fund for Scientific Research, Flanders; the K.U. Leuven; the VIB, Methusalem (K.U. Leuven and the Flemish government); the Foundation for Alzheimer Research (SAO/FRMA); and funding by the European Research Council (ERC). B.D.S. is the Arthur Bax and Anna Vanluffelen chair for Alzheimer's disease. U.M. was supported by grants from the German Research Foundation (DFG) [grant numbers MU1457/8-1 and MU1457/9-1].

Supplementary material available online at
http://jcs.biologists.org/lookup/suppl/doi:10.1242/jcs.122440/-/DC1

References

Aydin, D., Filippov, M. A., Tschäpe, J. A., Gretz, N., Prinz, M., Eils, R., Brors, B. and Müller, U. C. (2011). Comparative transcriptome profiling of amyloid precursor protein family members in the adult cortex. *BMC Genomics* **12**, 160.

Bai, Y., Markham, K., Chen, F., Weerasekera, R., Watts, J., Horne, P., Wakutani, Y., Bagshaw, R., Mathews, P. M., Fraser, P. E. et al. (2008). The in vivo brain interactome of the amyloid precursor protein. *Mol. Cell. Proteomics* **7**, 15-34.

Banker, G. and Goslin, K. (1988). Developments in neuronal cell culture. *Nature* **336**, 185-186.

Bergmans, B. A., Shariati, S. A., Habets, R. L., Verstreken, P., Schoonjans, L., Müller, U., Dotti, C. G. and De Strooper, B. (2010). Neurons generated from APP/APLP1/APLP2 triple knockout embryonic stem cells behave normally in vitro and in vivo: lack of evidence for a cell autonomous role of the amyloid precursor protein in neuronal differentiation. *Stem Cells* **28**, 399-406.

Calderon de Anda, F., Gärtner, A., Tsai, L. H. and Dotti, C. G. (2008). Pyramidal neuron polarity axis is defined at the bipolar stage. *J. Cell Sci.* **121**, 178-185.

Cao, X. and Südhof, T. C. (2001). A transcriptionally [correction of transcriptively] active complex of APP with Fe65 and histone acetyltransferase Tip60. *Science* **293**, 115-120.

Chanas-Sacre, G., Rogister, B., Moonen, G. and Leprince, P. (2000). Radial glia phenotype: origin, regulation, and transdifferentiation. *J. Neurosci. Res.* **61**, 357-363.

Chenn, A. and Walsh, C. A. (2002). Regulation of cerebral cortical size by control of cell cycle exit in neural precursors. *Science* **297**, 365-369.

Coksaygan, T., Magnus, T., Cai, J., Mughal, M., Lepore, A., Xue, H., Fischer, I. and Rao, M. S. (2006). Neurogenesis in Talpha-1 tubulin transgenic mice during development and after injury. *Exp. Neurol.* **197**, 475-485.

Deyts, C., Vetrivel, K. S., Das, S., Shepherd, Y. M., Dupré, D. J., Thinakaran, G. and Parent, A. T. (2012). Novel GαS-protein signaling associated with membrane-tethered amyloid precursor protein intracellular domain. *J. Neurosci.* **32**, 1714-1729.

Diez-Roux, G., Banfi, S., Sultan, M., Geffers, L., Anand, S., Rozado, D., Magen, A., Canidio, E., Pagani, M., Peluso, I. et al. (2011). A high-resolution anatomical atlas of the transcriptome in the mouse embryo. *PLoS Biol.* **9**, e1000582.

Feng, L., Hatten, M. E. and Heintz, N. (1994). Brain lipid-binding protein (BLBP): a novel signaling system in the developing mammalian CNS. *Neuron* **12**, 895-908.

Gloster, A., Wu, W., Speelman, A., Weiss, S., Causing, C., Pozniak, C., Reynolds, B., Chang, E., Toma, J. G. and Miller, F. D. (1994). The T alpha 1 alpha-tubulin promoter specifies gene expression as a function of neuronal growth and regeneration in transgenic mice. *J. Neurosci.* **14**, 7319-7330.

Goto, H., Tomono, Y., Ajiro, K., Kosako, H., Fujita, M., Sakurai, M., Okawa, K., Iwamatsu, A., Okigaki, T., Takahashi, T. et al. (1999). Identification of a novel phosphorylation site on histone H3 coupled with mitotic chromosome condensation. *J. Biol. Chem.* **274**, 25543-25549.

Hashimoto-Torii, K., Torii, M., Sarkisian, M. R., Bartley, C. M., Shen, J., Radtke, F., Gridley, T., Sestan, N. and Rakic, P. (2008). Interaction between Reelin and Notch signaling regulates neuronal migration in the cerebral cortex. *Neuron* **60**, 273-284.

Haubensak, W., Attardo, A., Denk, W. and Huttner, W. B. (2004). Neurons arise in the basal neuroepithelium of the early mammalian telencephalon: a major site of neurogenesis. *Proc. Natl. Acad. Sci. USA* **101**, 3196-3201.

Heber, S., Herms, J., Gajic, V., Hainfellner, J., Aguzzi, A., Rülicke, T., von Kretzschmar, H., von Koch, C., Sisodia, S., Tremml, P. et al. (2000). Mice with combined gene knock-outs reveal essential and partially redundant functions of amyloid precursor protein family members. *J. Neurosci.* **20**, 7951-7963.

Hébert, S. S., Serneels, L., Tolia, A., Craessaerts, K., Derks, C., Filippov, M. A., Müller, U. and De Strooper, B. (2006). Regulated intramembrane proteolysis of amyloid precursor protein and regulation of expression of putative target genes. *EMBO Rep.* **7**, 739-745.

Herms, J., Anliker, B., Heber, S., Ring, S., Fuhrmann, M., Kretzschmar, H., Sisodia, S. and Müller, U. (2004). Cortical dysplasia resembling human type 2 lissencephaly in mice lacking all three APP family members. *EMBO J.* **23**, 4106-4115.

Homayouni, R., Rice, D. S., Sheldon, M. and Curran, T. (1999). Disabled-1 binds to the cytoplasmic domain of amyloid precursor-like protein 1. *J. Neurosci.* **19**, 7507-7515.

Lakomá, J., Garcia-Alonso, L. and Luque, J. M. (2011). Reelin sets the pace of neocortical neurogenesis. *Development* **138**, 5223-5234.

Leyssen, M., Ayaz, D., Hébert, S. S., Reeve, S., De Strooper, B. and Hassan, B. A. (2005). Amyloid precursor protein promotes post-developmental neurite arborization in the Drosophila brain. *EMBO J.* **24**, 2944-2955.

López-Sánchez, N., Müller, U. and Frade, J. M. (2005). Lengthening of G2/mitosis in cortical precursors from mice lacking beta-amyloid precursor protein. *Neuroscience* **130**, 51-60.

Lorent, K., Overbergh, L., Moechars, D., De Strooper, B., Van Leuven, F. and Van den Berghe, H. (1995). Expression in mouse embryos and in adult mouse brain of three members of the amyloid precursor protein family, of the alpha-2-macroglobulin receptor/low density lipoprotein receptor-related protein and of its ligands apolipoprotein E, lipoprotein lipase, alpha-2-macroglobulin and the 40,000 molecular weight receptor-associated protein. *Neuroscience* **65**, 1009-1025.

Ma, Q.-H., Futagawa, T., Yang, W.-L., Jiang, X.-D., Zeng, L., Takeda, Y., Xu, R.-X., Bagnard, D., Schachner, M., Furley, A. J. et al. (2008). A TAG1-APP signalling pathway through Fe65 negatively modulates neurogenesis. *Nat. Cell Biol.* **10**, 283-294.

McConnell, S. K. and Kaznowski, C. E. (1991). Cell cycle dependence of laminar determination in developing neocortex. *Science* **254**, 282-285.

Molyneaux, B. J., Arlotta, P., Menezes, J. R. and Macklis, J. D. (2007). Neuronal subtype specification in the cerebral cortex. *Nat. Rev. Neurosci.* **8**, 427-437.

Müller, U. C. and Zheng, H. (2012). Physiological functions of APP family proteins. *Cold Spring Harb Perspect Med* **2**, a006288.

Müller, U. C., Pietrzik, C. U. and Deller, T. (2012). The physiological functions of the β-amyloid precursor protein APP. *Exp. Brain Res.* **217**, 325-329.

Nikolaev, A., McLaughlin, T., O'Leary, D. D. and Tessier-Lavigne, M. (2009). APP binds DR6 to trigger axon pruning and neuron death via distinct caspases. *Nature* **457**, 981-989.

Pechnick, R. N., Zonis, S., Wawrowsky, K., Pourmorady, J. and Chesnokova, V. (2008). p21Cip1 restricts neuronal proliferation in the subgranular zone of the dentate gyrus of the hippocampus. *Proc. Natl. Acad. Sci. USA* **105**, 1358-1363.

Reinhard, C., Hébert, S. S. and De Strooper, B. (2005). The amyloid-beta precursor protein: integrating structure with biological function. *EMBO J.* **24**, 3996-4006.

Roncarati, R., Šestan, N., Scheinfeld, M. H., Berechid, B. E., Lopez, P. A., Meucci, O., McGlade, J. C., Rakic, P. and D'Adamio, L. (2002). The γ-secretase-generated intracellular domain of β-amyloid precursor protein binds Numb and inhibits Notch signaling. *Proc. Natl. Acad. Sci. USA* **99**, 7102-7107.

Soba, P., Eggert, S., Wagner, K., Zentgraf, H., Siehl, K., Kreger, S., Löwer, A., Langer, A., Merdes, G., Paro, R. et al. (2005). Homo- and heterodimerization of APP family members promotes intercellular adhesion. *EMBO J.* **24**, 3624-3634.

Suzuki, T., Ando, K., Isohara, T., Oishi, M., Lim, G. S., Satoh, Y., Wasco, W., Tanzi, R. E., Nairn, A. C., Greengard, P. et al. (1997). Phosphorylation of Alzheimer beta-amyloid precursor-like proteins. *Biochemistry* **36**, 4643-4649.

Tabata, H. and Nakajima, K. (2001). Efficient in utero gene transfer system to the developing mouse brain using electroporation: visualization of neuronal migration in the developing cortex. *Neuroscience* **103**, 865-872.

Tabata, H. and Nakajima, K. (2008). Labeling embryonic mouse central nervous system cells by in utero electroporation. *Dev. Growth Differ.* **50**, 507-511.

Tamayev, R., Zhou, D. and D'Adamio, L. (2009). The interactome of the amyloid beta precursor protein family members is shaped by phosphorylation of their intracellular domains. *Mol. Neurodegener.* **4**, 28.

Temple, S. and Davis, A. A. (1994). Isolated rat cortical progenitor cells are maintained in division in vitro by membrane-associated factors. *Development* **120**, 999-1008.

Vidaki, M., Tivodar, S., Doulgeraki, K., Tybulewicz, V., Kessaris, N., Pachnis, V. and Karagogeos, D. (2012). Rac1-dependent cell cycle exit of MGE precursors and GABAergic interneuron migration to the cortex. *Cereb. Cortex* **22**, 680-692.

Visel, A., Thaller, C. and Eichele, G. (2004). GenePaint.org: an atlas of gene expression patterns in the mouse embryo. *Nucleic Acids Res.* **32 Database issue**, D552-D556.

Wang, Z., Wang, B., Yang, L., Guo, Q., Aithmitti, N., Songyang, Z. and Zheng, H. (2009). Presynaptic and postsynaptic interaction of the amyloid precursor protein promotes peripheral and central synaptogenesis. *J. Neurosci.* **29**, 10788-10801.

Weyer, S. W., Klevanski, M., Delekate, A., Voikar, V., Aydin, D., Hick, M., Filippov, M., Drost, N., Schaller, K. L., Saar, M. et al. (2011). APP and APLP2 are essential at PNS and CNS synapses for transmission, spatial learning and LTP. *EMBO J.* **30**, 2266-2280.

Yang, Y. T., Wang, C. L. and Van Aelst, L. (2012). DOCK7 interacts with TACC3 to regulate interkinetic nuclear migration and cortical neurogenesis. *Nat. Neurosci.* **15**, 1201-1210.

Yoon, K., Nery, S., Rutlin, M. L., Radtke, F., Fishell, G. and Gaiano, N. (2004). Fibroblast growth factor receptor signaling promotes radial glial identity and interacts with Notch1 signaling in telencephalic progenitors. *J. Neurosci.* **24**, 9497-9506.

Young-Pearse, T. L., Bai, J., Chang, R., Zheng, J. B., LoTurco, J. J. and Selkoe, D. J. (2007). A critical function for beta-amyloid precursor protein in neuronal migration revealed by in utero RNA interference. *J. Neurosci.* **27**, 14459-14469.

Young-Pearse, T. L., Chen, A. C., Chang, R., Marquez, C. and Selkoe, D. J. (2008). Secreted APP regulates the function of full-length APP in neurite outgrowth through interaction with integrin beta1. *Neural Dev.* **3**, 15.